

Article

Synthesis of Polyaluminum Chloride Coagulant from Waste Aluminum Foil and Utilization in Petroleum Wastewater Treatment

Hanan H. Youssef¹, Sherif A. Younis^{1,*}, Esraa M. El-Fawal¹, Hager R. Ali¹, Yasser M. Moustafa¹ and Gehad G. Mohamed^{2,3}

¹ Analysis and Evaluation Department, Egyptian Petroleum Research Institute, Nasr City 11727, Cairo, Egypt

² Chemistry Department, Faculty of Science, Cairo University, Giza 12613, Egypt

³ Nanoscience Department, Basic and Applied Sciences Institute, Egypt-Japan University of Science and Technology, New Borg El Arab 21934, Alexandria, Egypt

* Correspondence: sherifali_r@yahoo.com

Abstract: This work investigates the potential synthesis of cost-effective polyaluminum chloride (PACl) coagulant from waste household aluminum foil and utilization for treating petroleum wastewater (PWW), especially dissolved organic compounds (DOC, like octanol–water mixture) and nonsettleable suspended (NSS-kaolin) mineral particles. Based on the Standard Practice for Coagulation–Flocculation Jar Test, the efficiency of PACl for DOC and NSS removal was evaluated in relation to the effects of the operational parameters. The results demonstrated that the as-prepared PACl has an amorphous morphology with a Keggin-type e-Al₁₃ molecular structure $\left[\text{Na}\left[\text{AlO}_4(\text{OH})_{24}(\text{H}_2\text{O})\right] \cdot x\text{H}_2\text{O}\right]$ and good thermal stability up to 278 °C. PACl coagulant also exhibited a higher efficiency for NSS removal than DOC by around 1.5- to 1.9-fold under broad pH (5–7), while a higher acidic/alkaline pH disrupts the sweep floc formation. An increased PACl dosage (over 25 mg/L) also caused a decrease in the coagulation efficiency by 11.7% due to Al species' transformation and pH depression (from 6.8 to 4.9) via increased PACl hydrolysis. With a fast rotating speed of 280 rpm for 2 min, the minimum dose of PACl (10–25 mg/L) can maximize the removal efficiency of NSS (~98%) and DOC (~69%) at pH 6.5 ± 0.5 and 35 °C after 30 min of settling time. Treating actual saline PWW samples (salinity up to 187.7 g/L) also verified the high efficacy of PACl coagulation performance in reducing the turbidity and dissolved hydrocarbons by more than 75.5% and 67.7%, respectively. These findings verify the techno-economic feasibility of the as-prepared PACl coagulant in treating PWW treatment at different salinity levels.

Keywords: waste aluminum foil; polyaluminum chloride (PACl); turbidity; organic hydrocarbon; petroleum wastewater; coagulation treatment



Citation: Youssef, H.H.; Younis, S.A.; El-Fawal, E.M.; Ali, H.R.; Moustafa, Y.M.; Mohamed, G.G. Synthesis of Polyaluminum Chloride Coagulant from Waste Aluminum Foil and Utilization in Petroleum Wastewater Treatment. *Separations* **2023**, *10*, 570. <https://doi.org/10.3390/separations10110570>

Academic Editor: Qicheng Feng

Received: 2 October 2023

Revised: 8 November 2023

Accepted: 9 November 2023

Published: 15 November 2023



Copyright: © 2023 by the authors. Licensee MDPI, Basel, Switzerland. This article is an open access article distributed under the terms and conditions of the Creative Commons Attribution (CC BY) license (<https://creativecommons.org/licenses/by/4.0/>).

1. Introduction

Environmental pollution is a pressing global issue that poses significant challenges to the well-being of our planet and its inhabitants. Water pollution is a significant environmental concern among the various forms of pollution, posing a global threat to aquatic life and human health [1]. Specifically, the discharge of petroleum wastewater (PWW), also known as oilfield effluent, has been identified as particularly hazardous to the environment due to its toxic and complex chemical constituents. The chemical pollutants of PWW include dissolved organic compounds (DOC), emulsified oil hydrocarbons, inorganic salts, additive chemicals, and heavy metals (e.g., lead, mercury, cadmium) and insoluble (e.g., nonsettleable suspended mineral solids (NSS)), and polycyclic aromatic hydrocarbons (PAHs)) [2,3]. These petroleum pollutants can harm aquatic life and humans, even at low concentrations. It is also well known that the petroleum sector (e.g., oil fields, petrochemicals, and refineries) is among the most significant contributors to water pollution. The global production rate of PWW is around ~250 million barrels/day from oil and gas (O&G) fields during exploration, drilling, production, and transportation [3]. The daily released

PWW is projected to increase to 605 million barrels/day shortly due to the increased dependence on fossil fuel as a primary energy source [2]. However, the characteristics of PWW (i.e., inorganic and organic constituents) are widely varied, depending on the type/nature of the formation, reservoir lifetime, chemical injection, and operational technology [4]. Thus, undoubtedly, the direct disposal of untreated PWW without proper management can lead to severe environmental pollution, which, in turn, threatens human health and increases the scarcity of freshwater resources [5].

A typical PWW treatment plant consists of three major techniques: physical (primary), chemical (secondary), and advanced (tertiary) treatment technologies [6]. Note that the advanced/tertiary treatment methods (e.g., adsorption, photocatalysis, electrocatalysis, membrane separation, and biological techniques) are commonly utilized for enhanced purification of industrial effluents from dissolved chemical (organic and inorganic) pollutants based on the targeted purposes (e.g., enhanced oil recovery, irrigation, or industrial reuse). For instance, considering advanced oxidation technologies, many efforts have been made to explore innovative photocatalytic materials to accelerate the solar-driven photodegradation of varying organic pollutants in industrial effluent and partially solve water pollution problems [7]. However, the traditional methods are often used as a pretreatment step to prepare oily wastewater for secondary and advanced treatment processes. In this regard, traditional treatment methods (e.g., coagulation–flocculation) can destabilize and break emulsified organic matter and reduce suspended solids (e.g., sand and slit), which can block the light source or deactivate the catalyst's surface during the advanced oxidation treatment of oily wastewater. In particular, coagulation–flocculation technology is considered one of the essential treatment steps in all industrial wastewater treatment plants due to its ease of operation, low energy consumption, and economic effectiveness [8]. The chemical coagulation process also can treat large volumes of PWW generated daily [9]. It is commonly used as a secondary wastewater treatment/clarification step to reduce turbidity (e.g., NSS like fine mineral, sand, and clay particles) and DOC (free and dissolved fractions) via aggregation and flocculation mechanisms [10]. Nonetheless, one of the critical drawbacks of the chemical coagulation process is the low efficiency in removing emulsified organic/oil contents. In addition, emulsified oil can attach fine mineral particles (like clay colloids) in PWW, increasing the colloidal stability of NSS and water-soluble surface-active minerals during coagulation [5,11]. Consequently, numerous efforts have emphasized developing cost-effective chemical coagulants to treat PWW contaminated with dissolved/emulsified oil and nonsettleable fine mineral particles.

Numerous research efforts have been recently made to develop cost-effective and eco-friendly coagulants (inorganic and polymeric types) with high capacity to treat petroleum and oily wastewater at the minimum doses to avoid secondary pollution [12]. In particular, polynuclear-aluminum-based coagulants (e.g., polyaluminum chloride (PACl)) are known to be the most industrially used to improve electrostatic interactions between organic and particulate fractions to catalyze floc formation and the precipitation process. PACl has many benefits over other inorganic coagulants, including its simple preparation, high efficiency, lower sludge volume, minimum aluminum residual, and reduced effect on the raw water pH value. Polymeric PACl, which contains cationic species like $\text{Al}_2\text{O}_2(\text{OH})^+$ and Al_3O_4^+ , is among the least pH-sensitive coagulants because of (i) the high charge neutralization capacities of cationic alumina species and (ii) faster hydrolysis kinetics at a low and high alkalinity/basicity levels ($\% = 100/3 \times [\text{OH}]/[\text{Al}]$) [13]. To date, there have been many research studies on the coagulation behaviors of PACl for removing some natural organic matter (NOM)/humic substances (HS) [14,15] and mineral particulates [16] from deionized water solutions. These research studies have provided a better understanding of the coagulation mechanism and efficiency of PACl for NOM/HS removal. However, almost all research studies rely on conducting coagulation experiments in distilled/deionized water to summarize the aggregate reaction of PACl coagulant with NOM or mineral particles. Accordingly, it is still unclear whether this conclusion is valid for using PACl to treat all types of raw industrial water, like PWW effluent streams. In addition, the compatibility of

PACl in removing other types of hydrocarbon contaminants is not yet understood, except for the targeted NOM/HS (a typical organic pollutant) in the coagulation treatment [17].

Since the cost of coagulant production is a vital parameter in determining practical implementation in wastewater treatment, it is necessary to reduce the manufacturing cost of PACl to a minimum. In this regard, alumina solid waste is a particular environmental challenge due to its widespread occurrence and detrimental effects on ecosystems, public health, and natural resources. Since aluminum is the world's most frequently utilized non-ferrous metal daily, a large quantity (approx. over 150 million tonnes) of aluminum waste (e.g., alumina foil, dross, beverage cans, containers, etc.) is produced each year [18,19]. Exploiting these aluminum wastes has emerged as an industrial challenge due to their classification as hazardous waste for the environment [19]. This challenge can be addressed by incorporating a "win-win" sustainable solid waste management strategy. Reutilizing alumina solid waste to create value-added products like PACl for petroleum wastewater treatment can promote a circular economy and resource conservation, where resources are reused and recycled to minimize waste and environmental impact. This strategy also aligns with broader sustainability goals by committing to reducing environmental impacts and supporting sustainable practices. In fact, synthesizing PACl coagulant from a waste alumina foil could minimize the environmental burden associated with solid waste disposal. Compared with traditional aluminum extraction and energy-intensive PACl production methods, the eco-friendly synthesis of PACl from waste aluminum foil reduces the need for primary aluminum production and the associated greenhouse gas emissions [20]. Since PACl is known for producing less sludge than other coagulants, applying PACl for PWW treatment can further minimize disposal costs and its environmental impact. This is particularly advantageous when dealing with large volumes of petroleum wastewater generated daily, often containing large amounts of hydrocarbons. Accordingly, the recycling of waste aluminum foil for PACl synthesis and petroleum wastewater treatment could offer an innovative circular economy cycle by improving resource recovery and helping the petroleum sector meet increasingly stringent regulatory requirements for the discharge of oilfield wastewater into the natural environment (i.e., ensuring compliance with environmental standards).

On the above basis, this work focused on reutilizing waste aluminum foil as a raw aluminum source for manufacturing polyaluminum chloride (PACl) coagulant. Since waste aluminum foil is often readily available at a lower cost than traditional aluminum sources, the prepared PACl coagulant could increase the economic viability of coagulation treatment of petroleum wastewater through cost savings during the synthesis method. Accordingly, the as-prepared PACl powder was characterized using different techniques to evaluate its physicochemical properties and chemical composition. The effectiveness of PACl coagulant in treating petroleum wastewater was evaluated, especially towards removing DOC (in terms of octanol–water mixture) and turbidity (i.e., colloidal NSS-based kaolin mineral particulates). The coagulation efficiency of PACl in synthetic wastewater (salinity (NaCl) of 1000 mg/L) against the removal of NSS-kaolin mineral particulate and octanol (a typical model of polar DOC fraction) was investigated using a standard Jar test method. The effect of coagulation parameters on PACl efficiency for DOC/NSS removal rate was also studied and optimized, taking into account the role of the solution's pH, coagulant dosage, temperature, mixing speed, coagulation time, and settling time on the coagulation–flocculation mechanism. For the techno-economic feasibility study, the coagulation performance of PACl for treating three actual PWW samples (i.e., oilfield formation water) was also evaluated under optimized operation conditions to obtain insights into its applicability in a real-world field. Overall, this work can pave the way to reducing energy consumption associated with primary aluminum production, making the PACl synthesis process more energy efficient. Using waste aluminum foil can also allow for the customization of the PACl coagulant's properties to effectively remove oil, grease, and suspended solids from petroleum wastewater efficiently and economically.

2. Materials and Methods

2.1. Materials

Hydrochloric acid (HCl: 35–38%), sodium hydroxide (NaOH > 99%), sodium chloride (NaCl > 99%), and octanol (purity > 98%, a representative of polar/emulsified oil fraction) were purchased from Merck Co., Ltd. (Darmstadt, Germany). Commercial kaolin powder ($\text{Al}_2\text{Si}_2\text{O}_5(\text{OH})_4$: >97% purity) was purchased from an intermediate chemicals company in Egypt and used to represent colloidal NSS particles in water. Domestic aluminum foil wastes were collected from the local market. Deionized water (DI, 18.2 M Ω) was prepared at the Egyptian Petroleum Research Institute (EPRI). Three real PWW samples (Table 1) were received from the Central Analytical Lab (CAL) at EPRI for a case study.

Table 1. The physicochemical characteristics of three real PWW samples before and after coagulation treatment using PACl coagulant at optimum conditions.

Parameters	PWW-S1		PWW-S2		PWW-S3	
	Raw	Treated	Raw	Treated	Raw	Treated
pH	6.56	5.47	7.12	5.93	6.85	5.74
EC (mS/cm)	218.5	211.3	128.2	124.5	28.3	27.8
TDS (g/L)	196.1	193.4	104.5	102.67	21.56	20.97
Salinity (NaCl: g/L)	187.7	185.3	98.76	97.56	16.89	16.52
Hardness (CaCO_3 : mg/L)	26.46	25.27	21.87	21.11	19.87	19.54
Turbidity (NTU)	330	81 (75.5%)	248	47 (81.1%)	88	9.2 (89.8%)
DOC (mg/L)	285	92 (67.7%)	117	36 (69.2%)	54	17 (68.5%)

2.2. Synthesis of Poly Aluminum Chloride (PACl) Coagulant

Here, waste aluminum foil was used as a raw source of aluminum to prepare PACl coagulant, following the procedure described elsewhere with a slight modification in the synthesis method [21]. In a typical procedure, granular aluminum foil waste (10 gm) was first washed with hot DI to remove impurities and dust, then dried at 60 ± 10 °C. The dried aluminum foil was hydrolyzed with the aid of preheated HCl solution (35%, 100 mL at 65 ± 5 °C) under continuous stirring ($2\text{Al} + 6\text{HCl} + 12\text{H}_2\text{O} \rightarrow 2\text{AlCl}_3 \cdot 6\text{H}_2\text{O} + 3\text{H}_2$). In the next step, the aluminum chloride solution's reaction temperature was increased to 75 ± 5 °C under vigorous stirring (500 rpm) for 20 min. Under continuous stirring, the NaOH solution (1 M) was added dropwise to the above alumina solution mixture to reach a pH value of 9 ± 0.5 and achieve an OH/Al molar ratio of 2. These conditions stimulated the formation of polyaluminum chloride (PACl) coagulant as a white gel product. After 24 h of aging, the obtained PACl gel was separated via centrifugation (4233ECT laboratory centrifuge) and washed several times with DI, then dried at 85 ± 5 °C in an air oven for 12 h. The dried PACl powder was finally stored in a closed-cap glass bottle until further use for physicochemical characterization and coagulation study.

2.3. Jar Test Coagulation Experiment

Coagulation experiments were carried out using a bench-scale jar test apparatus (VELP Scientifica, JLT series, Usmate Velate (MB)-Italy) in a cylindrical container (1 L) under controlled operating parameters, following the standard Jar Test ASTM D-2035 method (ASTM = American Society for Testing and Materials) for the coagulation–flocculation process in the industrial wastewater treatment plants. Before each coagulation experimental run, a synthetic coagulation solution was freshly prepared by mixing the desired amount of washed kaolin fine powder (NSS fraction, particle size of <7.28 μm) and octanol (oil-based DOC fraction) in tap water (as a background solution) to achieve initial turbidity and oil concentration values of 270 NTU and 100 mg/L, respectively. Then, the salinity of the synthetic solution mixture was adjusted to 100 mg/L using NaCl salt and rapidly mixed (24 h) to stabilize the NSS-kaolin colloidal particles in the coagulation solution.

Based on the ASTM D-2035, the pH of the suspended coagulation solution was adjusted by injecting a predetermined volume of NaOH (0.01 M) or HCl (0.01 M) and mixed for 1 min. After that, a desired dosage of PACl coagulant was added, then subjected to a fast rotating speed of 120 rpm for 1 min, followed by slow mixing at 80 rpm for 30 min. The formed alum flocs were then left to settle for a specific time (30 min). Following the settling process, a 25 mL aliquot sample was taken from the treated water (approx. at 2–4 cm depth below the water surface) to evaluate water quality in terms of turbidity (a standard metric for NSS removal %), the solution's pH, conductivity (mS/cm at 25 °C), and dissolved octanol oil concentration. To optimize the PACl coagulation efficiency, the effect of the operational parameters on the removal efficiency of NSS (initial turbidity = 270 NTU) and dissolved octanol oil fraction (initial concentration = 100 mg/L) from synthetic wastewater was investigated. The operational parameters include the solution's pH (3–9), PACl coagulant dose (5–100 mg/L), the solution's temperature (10–55 °C), rapid mixing speed (120–360 rpm), rapid mixing time (1–5 min), slow mixing time (15 and 30 min), and settling time (5–30 min).

At optimum operating conditions, the coagulation performance of PACl for treating actual PWW samples (oilfield formation water, as a case study) was also investigated. The physicochemical characteristics of PWW before and after the coagulation treatment are summarized in Table 1, including total dissolved inorganic salts (TDS: g/L), electrical conductivity (EC: mS/cm), the solution's pH, water hardness, salinity (NaCl), oil content, and turbidity (NTU). The removal efficiency (RE) of DOC and NSS contents from synthetic wastewater was calculated using the following equation (Equation (1)).

$$\text{RE} (\%) = [(T_0 - T)/T_0] \times 100 \quad (1)$$

where, T_0 and T represent the concentration of DOC or NSS-kaolin before and after the coagulation treatment, respectively.

Water quality before and after the coagulation treatment was also evaluated by using the following instruments: (i) a portable turbidimeter (HACH: model 2100P) to determine the removal efficiency of NSS content, (ii) ERACHECK ECO oil-in-water analyzer (eralytics, Vienna, Austria) to evaluate the removal efficiency of DOC fraction (based on the standard method ASTM D- 8193), (iii) a pH/mV benchtop meter (JENWAY, model 3510) to monitor the change in the solution's pH, and (iv) a benchtop conductivity meter (WTW, model 3110) to determine water salinity.

2.4. Characterization Instruments

The physicochemical characteristics of the as-prepared PACl powder were evaluated using various techniques, such as X-ray diffraction (XRD), field emission-scanning electron microscope (FE-SEM), thermo-gravimetric analysis (TGA), N₂-adsorption/desorption isotherm, Fourier-Transform Infrared (FT-IR) spectroscopy, and dynamic light scattering (DLS). The XRD analysis was performed using an X-ray source (PANalytical XPERT PRO MPD, Almelo, The Netherlands) with Cu K α radiation (40 kV, 40 mA, $\lambda = 1.5418 \text{ \AA}$) over the 2 θ range of 0–80° at room temperature. The crystallographic standard database (JCPDS) identifies the crystal phase structure. The surface morphology and elemental composition of PACl coagulant were evaluated via the FE-SEM technique (Carl Zeiss Microscopy GmbH, sigma 300 vp, Oberkochen, Germany) attached with an Oxford energy-dispersive X-ray spectroscopy (EDX: Oxford Instruments PLC, Abingdon, UK) equipped with an 80 mm² X-Max detector. The N₂ adsorption–desorption isotherm of PACl was measured using a gas analyzer (model BELSORP max II, Bonsai advanced technologies, Madrid-Spain) at 77 K (note that the sample was degassed at 120 °C for 6 h before analysis). Based on the N₂ adsorption–desorption isotherm, the textural features (specific surface area (S_{BET})), total pore volume (V_t), and average pore diameter (d_p)) of PACl powder were determined. The surface chemistry (functional groups) of PACl was analyzed using FTIR spectroscopy (Perkin Elmer, Spectrum One, Shelton, CT, USA) at a wavenumber range of 4000–400 cm⁻¹. The thermal stability of PACl was evaluated using a thermogravimetric

analyzer (TGA/DSC: model SDT-Q600, USA) from the ambient temperature (25°C) to 800°C under atmospheric nitrogen with a heating rate of $10^{\circ}\text{C}/\text{min}$. The particle size distribution of PACl was also determined via dynamic light scattering (DLS: ZetaSizer Nano Series (HT), Malvern Panalytical, Malvern, UK). The surface zeta potential (ZP) of PACl precipitates was monitored using a Zeta Potential analyzer (Zetasizer Nano-ZS, Malvern Panalytical, Malvern, UK).

3. Results and Discussion

3.1. Characterization Data

Here, PACl powder coagulant was prepared from aluminum foil waste via the hydrolysis of aluminum salt (AlCl_3 , as Al^{3+} hydrate ions), following the formation of mono/multi-hydroxy Al complexes as inorganic polymers at a higher solution pH (NaOH). In these inorganic polymers, a bridging effect occurred between Al ions and the hydroxyl group ($2\text{AlCl}_3 + 6\text{NaOH} + \text{H}_2\text{O} \rightarrow [\text{Al}_2(\text{OH})_n\text{Cl}_{6-n}]_m + 6\text{NaCl}$).

Figure 1 shows the crystalline and surface functional characteristics of PACl powder via XRD and FT-IR analyses. From Figure 1a, the XRD pattern shows multiple diffraction peaks related to the presence of boehmite $\{\gamma\text{-AlOOH}$ at 2θ of 14.2° (020), 28.2° (120), 38.4° (140), 49.2° (200), and 64.1° (231)} and bayerite $\{\alpha\text{-Al(OH)}_3$ at 2θ of 18.6° (001), 20.3° (110), and 40.6° (201)} phases. This observation agrees with the formation of an amorphous PACl structure, with a Keggin-Al13(gl- ϵ -Al13) chemical formula of $\text{Na}[\text{AlO}_4(\text{OH})_{24}(\text{H}_2\text{O})]\cdot x\text{H}_2\text{O}$ (i.e., the active species in PACl). Additionally, PACl can exist as $[\text{Al}_2(\text{OH})_n\text{Cl}_{6-n}]_m$, where $m = 4\text{--}10$ and $n = 2\text{--}5$ [22,23]. In addition, the fairly low intensities of the diffraction peaks in the range of $2\theta > 27^{\circ}$ are also ascribed to the NaCl crystals (a by-product) produced during the hydrolyzation and polymerization of Al^{3+} hydrate ions [23]. In the FTIR spectrum (Figure 1b), the surface functionalities and chemical bonds formed during PACl preparation were also identified. In particular, the strong, wide bands at 3547 and 3427 cm^{-1} are assigned to the stretching vibrations of O-H (absorbed water) and Al-OH (PACl), respectively [24]. These FT-IR absorption peaks at 1639 , 1080 , and 618 cm^{-1} are also assigned to the O-H bending vibration (twisting, rocking, or wagging) in the structure of Al polycations [25], the asymmetric stretching vibration of Al-O-Al [24,26], and the vibration of the Al-O bond of the central AlO_4^- in the gl- ϵ -Al13 molecular structure, respectively [27]. In addition, the absorption band at 2148 cm^{-1} indicates the unsymmetrical stretching of water molecules coordinated with the gl- ϵ -Al13 molecules during the synthesis method [28]. Furthermore, the absorption band of the Al-O metal complex containing oxo and hydroxyl bridges characteristic of the Al polynuclear species in the PACl is observed at the regions $850\text{--}900\text{ cm}^{-1}$ [29]. These findings suggested the successful formation of PACl coagulant in which the Al-OH groups could play an essential role in the coagulation mechanism.

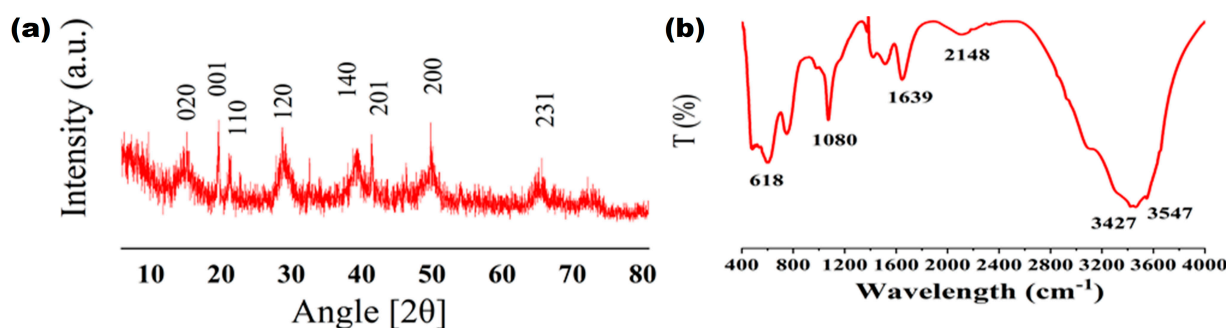


Figure 1. The characteristic patterns of PACl powder: (a) XRD pattern and (b) FTIR spectrum.

From the N_2 adsorption and desorption isotherm in Figure 2a, PACl exhibits a typical Type-IV isotherm with Type-H2 hysteresis loop (at $P/P_0 > 0.4$) according to the International Union of Pure and Applied Chemistry (IUPAC) classification. This indicates that PACl has ink-bottle-shaped porous structures containing both micropores and mesopores

in nature [30,31]. The pore size distribution profile (Figure 2b) of PACl coagulant also supported the micro/mesoporous nature of PACl in the range of 1.49 to 35 nm, with an average pore size (d_p) of 8.21 nm. The specific surface area (S_{BET}) and total pore volume (V_t) of the as-prepared PACl powder were also estimated at $60 \text{ m}^2 \cdot \text{g}^{-1}$ and $0.123 \text{ cm}^3 \cdot \text{g}^{-1}$, respectively. The TGA thermal analysis of PACl powder (Figure 2c) also demonstrated three decomposition stages with a total weight loss of 34% at 480 °C. The first stage showed a 9% decline in the PACl weight with a temperature rise from room temperature to 105 °C due to the physical desorption of water molecules from the PACl structure. In the second thermal degradation stage (105–278 °C), around 15% weight loss was recorded due to the evaporation of crystalline and chemically bonded/coordinated water molecules alongside chemically bonded Al-OH groups from the PACl surface. In the third stage (10% weight loss from 278 °C to 480 °C), the phase transition occurs via dehydration and incineration of PACl to the gibbsite/boehmite phase $\{\text{Al(OH)}_3\}/\text{AlO(OH)}$, then into aluminum oxide (Al_2O_3), as a final phase. These results agree with the endothermic peak at 264 °C observed in the DSC curve (Figure 2b), corresponding to the thermal decomposition of chemically bonded water and hydroxyl groups within the PACl structure [32].

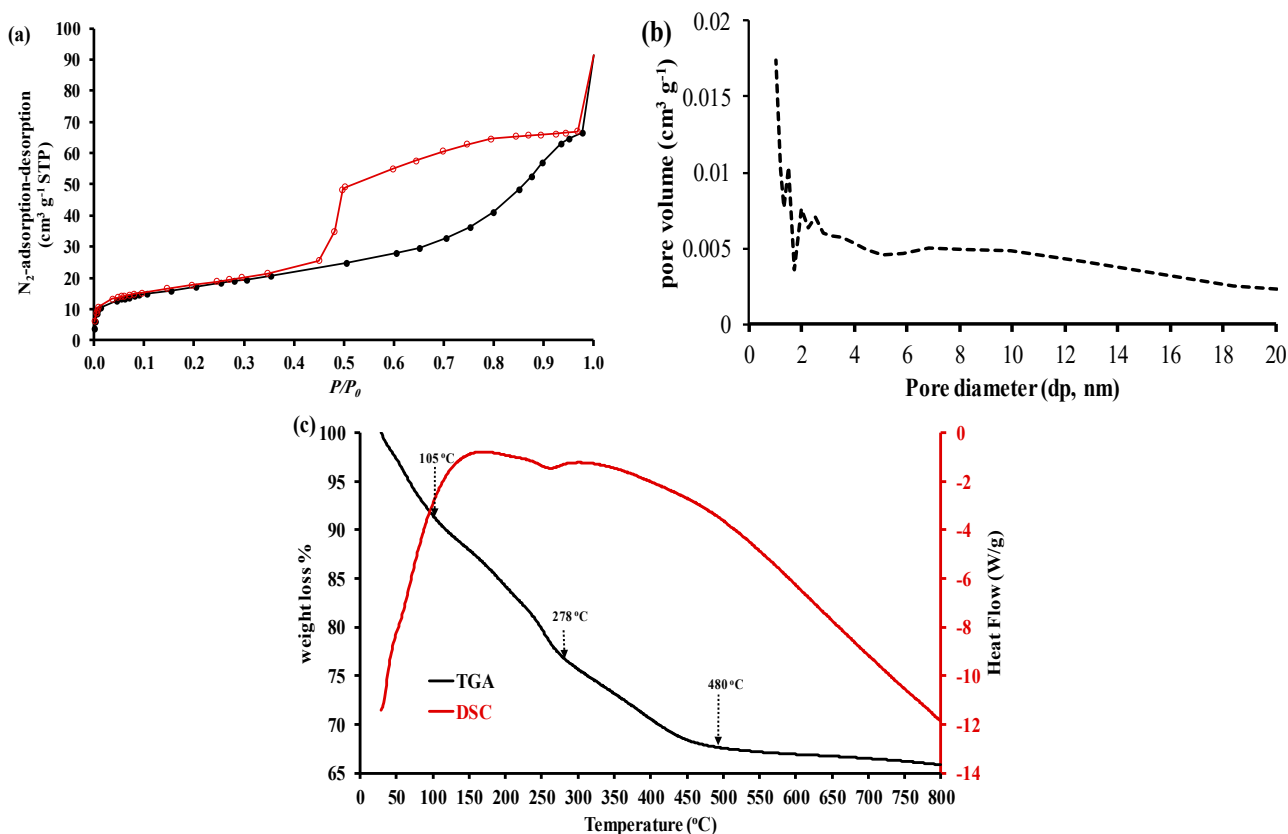


Figure 2. The textural and thermal properties of PACl powder: (a) N_2 adsorption–desorption isotherm, (c) pore size distribution profile, and (b) TGA/DSC curves under N_2 atmosphere.

Figure 3 presents the FE-SEM micrograph associated with EDX-elemental mapping of PACl powder and particle size distribution via DLS analysis. The FE-SEM image in Figure 3a shows that the PACl particles typically appear as irregularly shaped agglomerates (or aggregate clusters) with angular and rounded edges, forming larger-size particles from nanoscale to microscale in diameter. These agglomerated particles appeared as dense, compact clusters of smaller particles interconnected through porous networks. The surface of PACl particles exhibited a rough, non-uniform texture (amorphous), often associated with the amorphous structure of aluminum hydroxide compounds formed during the synthesis procedure. EDX-elemental maps in Figure 3b–f also demonstrate the uniform

distribution of Al, Cl, O, and Na ions in the PACl composition with % weight ratios of 51%, 6%, 39%, and 4%, respectively. Besides, all elemental constituents (Na, Cl, O, and Al dots) were distributed together within the PACl powder (inset Figure 3b), confirming the synthesis of Keggin–Al13 $\{\text{Na}[\text{AlO}_4(\text{OH})_{24}(\text{H}_2\text{O})]\cdot x\text{H}_2\text{O}\}$ as verified via XRD analysis. Based on the DLS histogram (Figure 3g), PACl has a particle size distribution of 295 to 715 nm range, with an average hydrodynamic particle diameter of 459 nm. The variation in the PACl size distribution can be attributed to the effect of an aqueous solution on the degree of aggregation and dispersion of PACl particles during DLS analysis.

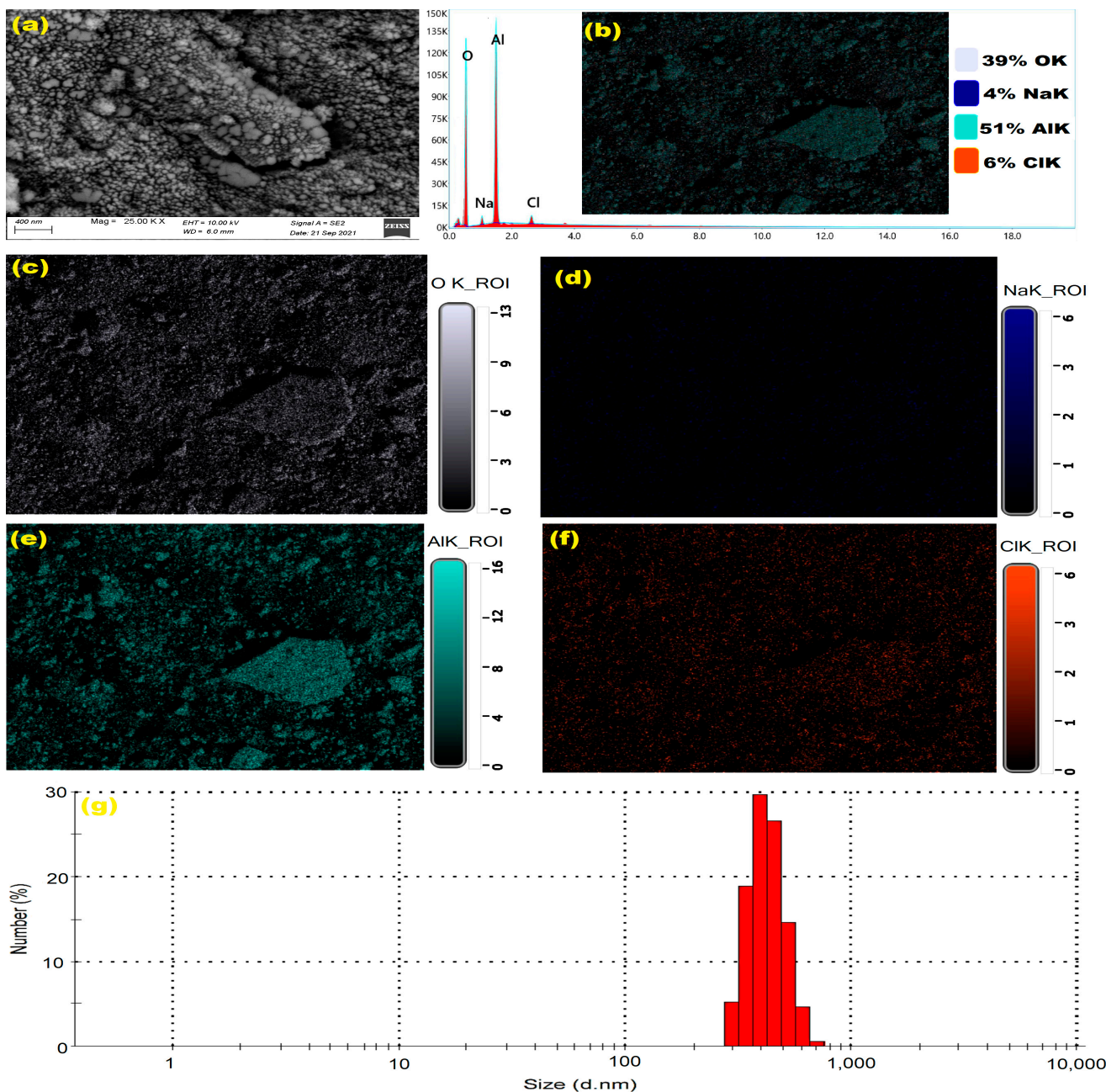


Figure 3. The morphological features of PACl powder: (a) FE-SEM image, (b–f) EDX-elemental mapping ((b) EDX-mapping spectra with (c) O, (d) Na, (e) Al, (f) Cl), and (g) DLS histogram.

3.2. Effect of Operation Conditions on the PACl Coagulation Efficiency

It is well known that tailoring coagulation conditions to the unique composition of the wastewater ensures an efficient and effective treatment. In this regard, various operational variables (e.g., solution pH, PACl dosage, mixing intensity/time, and temperature) can

significantly influence the effectiveness of PACl coagulant in wastewater treatment (e.g., NSS and oil removal). This is mainly ascribed to the critical role of water chemistry (i.e., operational variables) in charge neutralization, coagulant flocs' formation and their interaction with NSS and oil droplets, coagulation kinetics, flocs' settling rate, and sludge production during the treatment process. Hence, understanding and optimizing these operational variables based on the characteristics of the PWW are essential for maximizing PACl coagulation performance in a real field.

3.2.1. Solution pH

It is well known that water alkalinity/pH significantly affects Al-based coagulation efficiency by controlling a “sweep floc” formation (i.e., hydrolysis/polymerization of PACl (bridge aggregation)) and colloidal stability of solid particles (charge neutralization and precipitation). Accordingly, the relationship between the initial solution's pH (3–9) and PACl-based coagulation efficiency for NSS-kaolin and DOC removal was investigated and plotted in Figure 4. It seems that PACl has a vast working pH range with a highly stable NSS-kaolin (turbidity) and DOC removal capacity at a wide pH range of 4.0 to 7.0. In particular, PACl demonstrated a higher efficiency in removing NSS-kaolin than DOC matter at all tested pH conditions. The highest NSS-kaolin removal efficiency (average of $79.82 \pm 1.75\%$) was observed at pH 7.0 (Figure 4a). Compared to pH 7.0, the PACl coagulation performance against NSS-kaolin removal decreased sharply by 12.5% upon increasing the solution's pH to 9.0. Likewise, the DOC removal efficiency using PACl coagulant increased with a rise in the solution's pH from 3.0 to 6.0, then gradually declined at higher pH levels (alkaline solution conditions). The maximum DOC removal efficiency was 48.8% at pH 6.0 (Figure 4a). Hence, the coagulation efficiency of PACl for NSS and DOC removal can be optimized at neutral pH (6.0–7.0), which agrees with the reported optimums for Al-based coagulants [33,34].

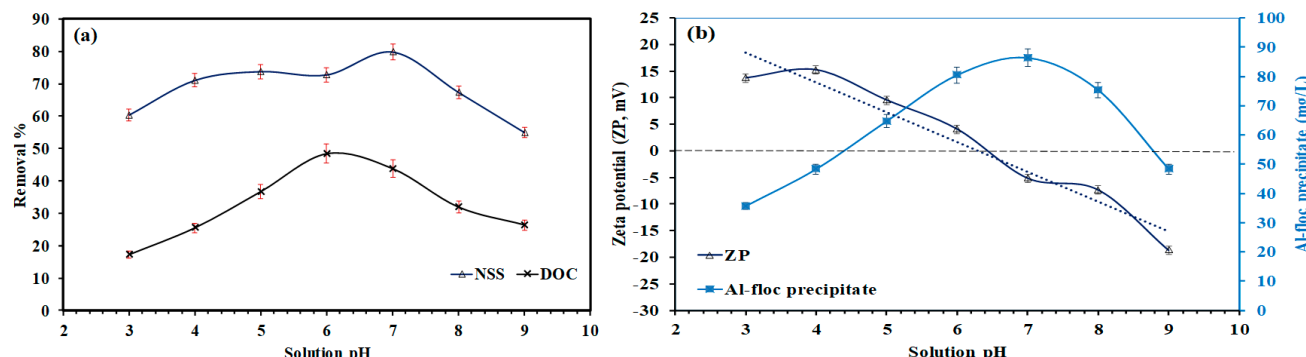


Figure 4. Effect of water solution pH on PACl coagulation properties: (a) NSS-kaolin turbidity and DOC organic matter removal efficiency and (b) the formation and zeta potential (ZP) of PACl floc precipitates.

Note that the typically higher efficiency of PACl for NSS removal compared to DOC matter could be explained in several ways. Coagulants like PACl work through charge neutralization on the particles' surface by forming aluminum hydroxide flocs in the water. Since PACl effectively neutralizes the negative charges on particles, almost all NSS particles have a net negative charge. Such phenomena can be explained based on the determined zeta potential (ZP: mV) of PACl precipitates (mg/L) as a function of the solution's pH (Figure 4b). As can be seen, the ZP of alum flocs formed after coagulation also shifted from the positive into the negative side as the initial pH increased from 3.0 to 9.0 (Figure 4b). In the acid region, the ZP of PACl-based flocs moved into a higher positive side, recording +13.6 mV (at pH = 3) due to the possible formation of positive PACl hydrolyzates in solutions such as Al(OH)_2^+ , $\text{Al}_2(\text{OH})_2^{4+}$, and $\text{Al}_3(\text{OH})_4^{5+}$. The higher hydronium (H^+) ions at acidic conditions also negatively impacted the degree of PACl polymerization by affecting the hydroxyl ($\text{Al}-\text{OH}-\text{Al}$) and oxygen ($\text{Al}-\text{O}-\text{Al}$) bridges. These positively

charged PACl hydrolyzates might adsorb on the negatively charged NSS-kaolin particles, destabilizing the colloidal stability and the “sweep floc” growth. As pH increases, the ZP of PACl-based flocs increases to the negative side, with the highest negative ZP value of -18.7 mV at $\text{pH} = 9.0$. At alkaline pH, the higher hydroxyl ($-\text{OH}$) ions also promoted the formation of Al(OH)_4^- hydrolyzate, decreasing the alum flocs’ stability. This observation is associated with a decline in alum flocs precipitate formation through an increase in the repulsion forces between negatively charged NSS-kaolin particles and ionized PACl forms (Al(OH)_4^- and AlO^-) in the solution. Such a charge neutralization mechanism increased the colloidal stability of NSS-kaolin in the water solution, leading to a decline in coagulation efficiency [35,36]. This indicated that the charge neutralization effect of PACl on an acid solution was superior to that in an alkaline solution. At near-neutral pH of 6.5 ± 0.5 , the charge neutralization is observed (ZP of $+4.05$ to -5.17 mV at 25°C), indicating the formation of a strong coagulation–flocculation (ZP range of $\pm 5\text{ mV}$) as per the recommendation of the ASTM method D1293-84(90). This means that coagulation zones (i.e., charge neutralization and stabilization) are observed at near-neutral pH as verified by an increase in the alum floc precipitates (76.6 to 86.3 mg/L) and a decline in the ZP values to the minimum ($+4.05$ to -7.35 mV). Accordingly, the alum flocs can physically attract and entrap NSS particles (e.g., solids and colloidal matter) by neutralizing surface negative charges, leading to the aggregation of NSS into larger, settleable flocs. In addition, it should be noted that the larger size and higher density of NSS particles make them more amenable to coagulation and settling than DOC matter, which typically exists as smaller, dissolved molecules in a solution. Hence, the limited interaction of PACl with DOC matter (compared to NSS-kaolin) can be ascribed to their higher dissolution in the water phase, and it may not readily interact or adsorb with the alum flocs (i.e., organic compounds are not readily settling out of the water on their own). Hence, the charge neutralization and stabilization zone of the floc would be observed through a decrease in the electrophoretic mobility of flocs when the respective ZP value is around $\pm 5\text{ mV}$ at 25°C due to the possible formation of polymeric Al-hydrolyzates (Al(OH)_3) in the solution [14,33]. These polymeric Al-hydrolyzates could attract NSS-kaolin and DOC matter, allowing for the co-precipitation and adsorption settling of NSS and DOC with Al-based floc precipitates in an aqueous solution. In this way, the effect of the solution’s pH depends on the balance between the reactions of DOC-kaolin particle functional groups with hydrolyzed Al(III)-based PACl coagulant in the aqueous solution. In addition, it is essential to note that coagulation is often targeted to purify water from particulate matter, not dissolved organic and inorganic compounds [18,23]. Thus, the coagulation removal of DOC matter is mainly a secondary consideration and may require additional treatment steps, such as biological or advanced oxidation processes, depending on the specific wastewater quality requirements. Therefore, depending on the application goals, a combination of treatment processes may be employed to effectively remove NSS and DOC contaminants in the actual PWW sample.

3.2.2. PACl Coagulant Dosage

The dosage of PACl coagulant plays a crucial role in turbidity and DOC removal efficiency from synthetic wastewater samples. At near-neutral pH (6.5 ± 0.5), the effect of PACl coagulant dosage (5–100 mg/L) on the removal efficiency of NSS-kaolin and DOC from synthetic water is shown in Figure 5. As can be seen, the removal efficiency of NSS-kaolin and DOC was negligible ($\leq 3\%$) in the absence of PACl (at zero dosage). In the presence of PACl coagulant, the coagulation efficiency of NSS-kaolin and DOC significantly increased with an increase in the PACl dosage, recording the maximum NSS-kaolin removal of $85.1 \pm 1.9\%$ at 10 to 25 mg/L PACl and near-neutral conditions. As PACl dosage increases to 100 mg/L, the removal efficiency of NSS-kaolin slightly decreases to 73.4%. Likewise, the maximum removal efficiency of DOC (52.8%) was observed at 25 mg/L PACl dosage. However, the higher PACl dose significantly presented an exciting phenomenon in organic pollution remediation. Specifically, the DOC removal efficiency decreased by half as the PACl dosage increased from 25 to 100 mg/L (Figure 5a). In Figure 5b, the change in dissolved Al(III)

ions for PACl shows an opposite trend to the removal efficiency of NSS-kaolin/DOC from the water solution. The dissolved Al(III) ions increased gradually from 0.18 to 2.73 mg/L with an increase in PACl dose from 25 to 100 mg/L. Such an increase in PACl dosage (up to 100 mg/L) also significantly contributed to the maximal pH depression from 6.8 to 4.98, reducing the coagulation's performance (Figure 5a,b). This phenomenon is attributed to the higher consumption of water alkalinity during the Al species' transformation process via PACl hydrolysis [37]. Above 25 mg/L PACl, the positively charged Al-based hydrolyzates also became more dominant, increasing the repulsion between the flocs and NSS-kaolin-coated DOC particles (i.e., interpret coagulation mechanism) [21,38]. In contrast, at a lower PACl dosage, the solution's pH was not significantly altered. Accordingly, the formed polymeric Al(OH)₃ floc could enhance the complexation of Al ions with floc precipitates [39,40]. This process could induce a fast charge neutralization and co-precipitation/adsorption of Al ions on NSS-kaolin/DOC particles while settling Al-based floc precipitates (see Figure 4). These observations showed that the optimization of PACl dosage is a critical operational parameter in the coagulation process due to its effect on Al speciation, floc growth, and coagulation mechanisms.

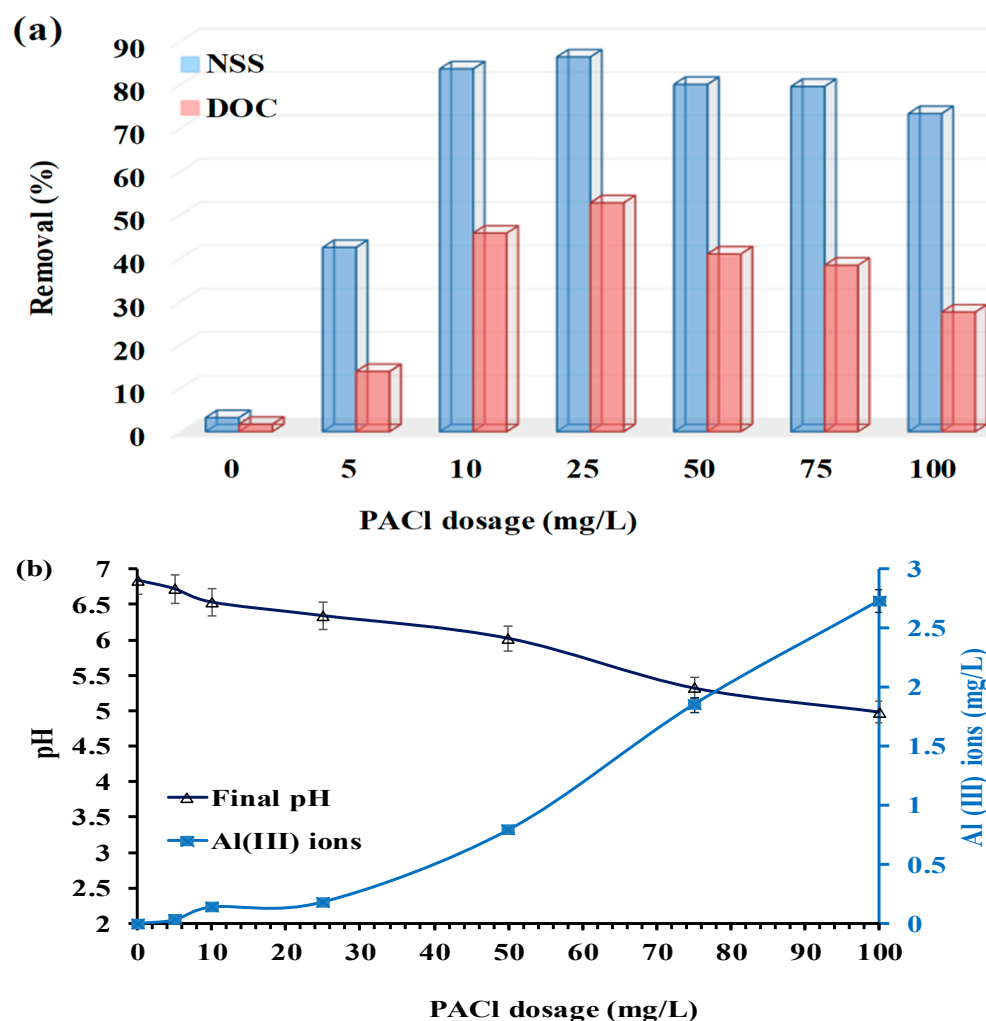


Figure 5. Effect of PACl coagulant dosage on the coagulation efficiency in terms of (a) NSS/DOC removal efficiency and (b) dissolved Al(III) ions versus final solution pH.

3.2.3. Solution Temperature

Temperature is among the essential factors significantly influencing coagulation efficiency through the control of PACl hydrolysis, shear break-up water viscosity, organic solubility, floc size, and strength [41]. Figure 6 illustrates the PACl coagulant's performance

for NSS-kaolin and DOC removal as a function of the solution's temperature. As shown in Figure 6, the NSS-kaolin removal efficiency enhanced (from 81.07 to 92.65%) with an increase in the solution's temperature from 15 to 35 °C, and then showed a declining trend with a further temperature rise to 55 °C (efficiency = 64.6%). In comparison, the coagulation efficiency of PACl for DOC removal was found to be stable (at $52.3 \pm 1.45\%$) over the temperature range of 15–35 °C. Following that, the removal efficiency of DOC sharply declined to 18.6% with an increase in temperature to 55 °C. As a matter of fact, the coagulation performance of PACl for NSS-kaolin and DOC removal had no noticeable difference over a temperature range of 25 to 35 °C, indicating that the growth of alum floc is favorable at room temperature (25 to 35 °C) and during the coagulation process. The slight decline in the coagulation efficiency of PACl for NSS-kaolin at low temperatures could be ascribed to the slight increase in water viscosity (unfavorable for the coagulation–flocculation process), causing a low collision between particles and reducing the rate of floc formation [42,43].

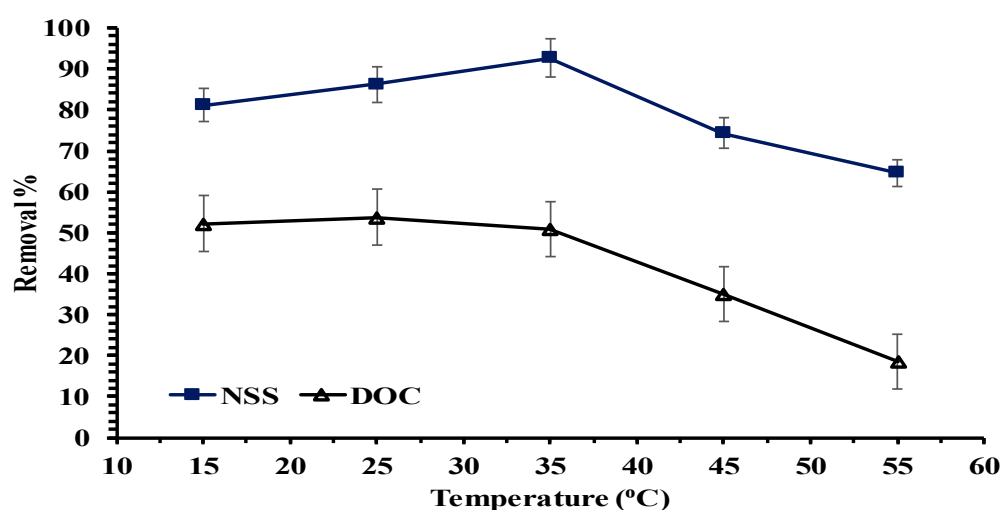


Figure 6. Effect of solution temperature on the coagulation efficiency of PACl (25 mg/L) for NSS-kaolin and DOC removal at $\text{pH } 6.5 \pm 0.5$.

In contrast, warmer water could accelerate the in situ hydrolysis rate of PACl during the coagulation, increasing the electrophoretic mobility and forming a larger alum floc that breaks quickly [41,44]. The smaller flocs decrease the rate of NSS-particle aggregation and floc settling than those obtained at room temperature. In addition, the increased solubility of DOC organic fraction at high temperatures may synergistically enhance the colloidal stability of NSS-kaolin in an aqueous solution, contributing to the lower coagulation efficiency.

3.2.4. Jar Test Mixing Speed and Time

Mixing conditions (fast/slow speed and time) are critical parameters affecting the flocs' formation and the performance of coagulation–flocculation reactors. The mixing (rotating) speed involves fast mixing to allow for charge neutralization (or polymer bridging) and the aggregation of colloidal particles, followed by slow mixing to stimulate floc growth and the settling processes [45,46]. Figure 7 shows the PACl coagulant performance for NSS-kaolin and DOC removal in relation to the effect of jar test operations (e.g., fast mixing speed (120–360 rpm) alongside the time of fast mixing (1–5 min), slow mixing (15–30 min), and settling (5–30 min)). Figure 7a shows that the NSS/DOC removal efficiencies significantly depend on a fast mixing speed and mixing time. The highest coagulation efficiency for NSS-kaolin (93.8%) and DOC (58%) was observed at 280 rpm for 2 min, which agrees with the standard operational limit. In addition, it was noted that prolonged mixing speed time (up to 5 min) had no significant effect on DOC removal but considerably declined NSS's removal efficiency by around 26%. An increased speed rate and time can stimulate the

breakdown from a large to a smaller floc size (i.e., floc rupture at higher velocity gradient and flocs erosion at prolonged mixing time) [45]. A very short mixing time (<2 min) also lowered the coagulation efficiency due to insufficient bridging formation of alum floc, reducing aggregates and collision between DOC/NSS-kaolin particles in the solution [47]. During the slow mixing speed (at 80 rpm), the DOC removal slightly increased from 58.7% to 62.5% by increasing the slow mixing time from 15 to 30 min (Figure 7b). However, in the case of residual turbidity, the slow mixing time showed no significant effect on the removal efficiency of NSS-kaolin (93.8–94.1%). An increased slow mixing time (from 15 to 30 min) also promotes the destabilization of the floc particles, enhancing the agglomeration of organic fraction and forming large flocculated particles (i.e., increased precipitates) [41]. Likewise, the removal of NSS/DOC increases by around 5.0/12.8% as the settling time increases from 5 to 30 min. The maximum removal efficiency of NSS-kaolin and DOC was 98.0% and 69.8%, respectively, after 30 min of settling time (Figure 7b). That is ascribed to the settling behavior of suspended particles and other organic floc particles collected during their movement in the bulk solution (formed settled particles) [48]. The above data suggest that the PAcI coagulation mechanism could involve the curling and bridging of polymeric alumina coupled with charge neutralization, while DOC probably accelerates the polymeric network produced by PAcI. Accordingly, the co-presence of DOC could play a key role in stabilizing the formed alum floc and enhancing the coagulation efficiency for NSS-kaolin removal (i.e., improving water clarification).

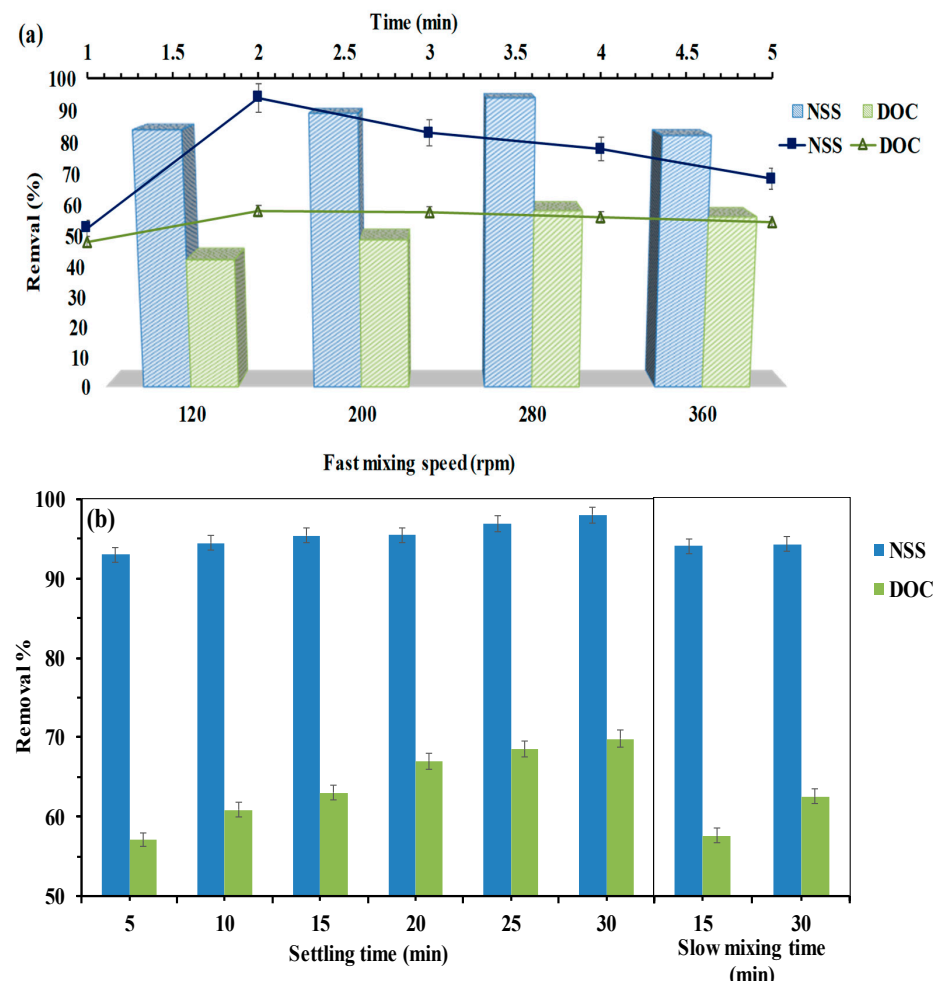


Figure 7. Effect of jar test operational parameters on PAcI coagulation efficiency: (a) speed mixing process (rate and time) and (b) settling time vs. slow mixing time.

3.3. Application Case Study: Real PWW Effluent Treatment

The above experimental studies revealed that the optimum coagulation conditions to achieve the maximum efficiency of PACl for DOC and NSS removal are as follows: pH 6.5 ± 0.5 , PACl dosage of 25 mg/L, temperature 35 °C, fast mixing speed (280 rpm for 2 min), low mixing speed (80 rpm for 30 min), and settling time 30 min. At these optimum conditions, the effectiveness of PACl coagulant was investigated for the treatment of three actual PWW samples (as a case study), as shown in Table 1. Before the coagulation treatment, it was noted that the organic, inorganic, and suspended constituents of the three PWW samples were remarkably varied. In particular, the results showed that the change in the EC and TDS values of PWW samples before and after the coagulation treatment was insignificant (<4.5%), indicating the negligible effect of PACl coagulant on the inorganic components of all PWW samples. However, it was noted that PACl coagulant exhibited a higher efficiency for suspended matter (turbidity) removal (efficiency 75.5–89.8%) than for the removal of hydrocarbon constituents (efficiency 67.7–69.2%). In addition, the efficiency of PACl for turbidity removal significantly depends on PWW salinity (i.e., total dissolved inorganic salts), showing a decline in efficiency by 14.3% with an increase in the EC value from 28.3 (PWW-S3) to 218.5 mS/cm (PWW-S1, Table 1). This means that an increased water salinity can interfere with the coagulation process of suspended particles.

In comparison, oil removal efficiency is independent of water salinity. This phenomenon might be attributed to the effect of inorganic constituents on charge neutralization, intraparticle bridging, and the electrostatic attractions between oil and PACl coagulant molecules (flocculation phenomena). Specifically, the higher dissolved salts (e.g., divalent cations like Ca^{2+} and Mg^{2+} in PWW) can compete with PACl for the available charges on oil droplets and suspended solids [13,17]. Excess metal ions at high salinity can also limit the availability of aluminum ions for the coagulation process. This competition reduces the effectiveness of PACl in neutralizing the charges on organic and suspended particulate matter. In addition, higher salinity can destabilize alum flocs by disrupting the hydroxyl ($\text{Al}-\text{OH}-\text{Al}$) and oxygen ($\text{Al}-\text{O}-\text{Al}$) bridges and reducing the electrostatic interactions that hold them together [35,36]. The water osmotic effect at high salinity can further influence alum coagulant flocs' swelling/shrinking behavior, impacting their stability and settling characteristics (i.e., less effective at capturing and settling oil droplets and suspended solids). In this case, the high ionic strength can enhance the dissolution of alum flocs formed, reducing their capacity to capture oil and solids. As a result, the flocs may disintegrate, and the agglomerated particles become more dispersed, reducing the overall coagulation efficiency [17]. To this end, it should be noted that if PWW salt contents affect the hydrolysis of Keggin-type e-Al₁₃ polycation and PACl coagulation mechanisms, particle destabilization will be adversely affected at high salinity due to the decrease in aggregation and settlement rate of alum flocs during the coagulation–flocculation process. The above results indicated the applicability of PACl prepared from waste aluminum foil in effectively removing suspended and organic contaminants from actual PWW samples with varying salinity levels.

Overall, the research findings demonstrated that scalability in the waste alumina foil-driven PACl coagulation treatment of oilfield wastewater is achievable but requires careful planning, monitoring, and adaptation to account for the specific challenges posed by the larger volume and variability of oilfield wastewater composition. In other words, the scalability of PACl in the coagulation treatment of oilfield effluent can face several challenges, primarily due to the complexity and variability of the wastewater composition. Particularly, the PACl should be able to adapt to high coagulation efficiency for oil and solid matter removal under fluctuations in oil content, salinity, pH, and other emulsified chemicals and contaminants (as explained earlier in Section 3.2). For example, the oilfield's high wastewater salinity and dissolved solids can limit the effectiveness of PACl. Hence, scaling up PACl-based coagulation processes may necessitate pre-treatment steps (such as desalination or dilution) to reduce the oilfield's wastewater salinity (i.e., ionic strength) and mitigate its negative impact on PACl coagulation performance. As treatment

capacity increases, the PACl dosing, mixing, and flocculation equipment should be scaled accordingly. However, optimizing a large-scale coagulation system can be a logistical challenge when dealing with large discharged volumes of oily contaminated wastewater with varying chemical characteristics. Thus, collaboration between engineers, chemists, and environmental professionals is crucial to designing and operating efficient and effective large-scale coagulation treatment systems.

4. Conclusions

This research study demonstrated the feasibility of recycling waste aluminum foil as a raw source for preparing cost-effective PACl coagulant to clarify petroleum wastewater from NSS matter and DOC contaminants. Characterization data verified the successful synthesis of amorphous PACl powder (average particle size of 458 nm) with a chemical composition of 51% Al, 39% O, 6% Cl, and 4% Na (a Keggin-type e-Al₁₃ molecular structure of $\text{Na}[\text{AlO}_4(\text{OH})_{24}(\text{H}_2\text{O})]\cdot\text{xH}_2\text{O}$). Based on the jar test studies, PACl exhibited a higher potential to remove NSS than DOC at a broader pH range (5–7) and room temperature. However, the efficiency of PACl significantly declined at alkaline pH and high salinity (ionic strength) due to the water osmotic effects on charge neutralization and alum floc stability. At the optimum conditions (pH: 6.5 ± 0.5 , temperature: 35 °C, settling time: 30 min, and fast speed: 280 rpm for 2 min), more than 98% of NSS and 69.8% of DOC contaminants can be removed by using a lower dosage of PACl (25 mg/L) coagulant. The coagulation efficiency of PACl depends greatly on solution temperature, pH, and jar test operation conditions, which control alum flocs' formation and settlement mechanisms. In addition, the polar organic contaminants could aid the bridging mechanism of polymeric alumina floc under controlled solution pH. As a case study, PACl showed high efficiency in treating actual PWW with varying salinity/TDS levels. A maximum removal efficiency of ~90% turbidity and 69% dissolved oil hydrocarbons can be achieved if the TDS of PWW is less than 17 g/L. However, it is essential to note that while the advantages of using waste aluminum foil for PACl production are promising, the specific benefits may depend on the quality and characteristics of the waste aluminum foil, the efficiency of the synthesis process, and the treatment goals for petroleum wastewater.

Overall, using PACl derived from waste aluminum foil in the oil industry can have environmental and economic implications. Some potential considerations for both aspects are as follows: (i) Recycling aluminum foil to produce PACl reduces the need for traditional aluminum production from bauxite, contributing to resource conservation and minimizing the associated environmental and health risks of primary aluminum production and landfills/incineration of waste alumina. (ii) Applying PACl in oilfield wastewater treatment may help improve water quality and environmental protection, which is particularly important in oilfield operations. (iii) As sustainability practices and environmental responsibility become increasingly crucial in the oil industry, adopting eco-friendly coagulants like PACl from recycled sources (e.g., waste aluminum foil) may align with evolving market and industry trends. Because the availability of waste aluminum foil is relatively stable compared to traditional aluminum sources, which are subject to price volatility and market fluctuations. Accordingly, PACl can be used as a favorable low-cost coagulant in the pretreatment of oilfield wastewater before being discharged or reused in enhanced oil recovery. Nonetheless, it is critical to note that the specific environmental and economic implications can vary depending on the scale of production, the availability of recycled aluminum foil, the efficiency of the recycling process, and the overall sustainability practices of the oil industry. Assessing the full range of implications, conducting a life-cycle analysis, and considering the broader environmental and economic context are essential when evaluating the use of PACl from recycled aluminum foil in the oil sector. Therefore, further research and development are needed to optimize the process and fully assess its advantages in the real oilfield industry. For instance, future research studies should explore sourcing high-quality recycled aluminum foil to ensure consistent PACl production by minimizing impurities in recycled aluminum wastes. In addition, it is vital to conduct

pilot-scale studies within oilfield operations to assess the real-world performance and efficiency of recycled aluminum-derived PACl (compared with traditional coagulants) in different oilfield environments and conditions to verify its potential for actual application. Research in these directions can help overcome the environmental and economic implications of adopting PACl from recycled aluminum foil in the oil industry. By addressing these challenges, researchers can contribute to more sustainable and responsible practices within the sector while maintaining the necessary performance standards for petroleum wastewater treatment.

Author Contributions: H.H.Youssef: Methodology, Investigation, Data Analysis and Writing—Original Draft; S.A.Younis: Conceptualization, Methodology, Investigation, Supervision, Validation, Resources, Data Curation, Formal analysis, Visualization, Project Administration, Writing—Original Draft and Reviewing and Editing; H.R.Ali and E.M.El-Fawal: Conceptualization, Methodology, Supervision, Resources, Formal analysis, Validation and Reviewing—Editing; Y.M.Moustafa and G.G.Mohamed: Supervision, Resources and Reviewing—Editing. All authors have read and agreed to the published version of the manuscript.

Funding: This research was funded by a grant from the Academy of Scientific Research and Technology (ASRT, Egypt) under Scientists for the Next Generation (SNG: Cycle 6—Section “Water management and rationalization”).

Data Availability Statement: The authors declare that the data supporting the findings of this study are available within the article.

Acknowledgments: The authors acknowledge the financial support given by Academy of Scientific Research and Technology (ASRT, Egypt), along with the technical support of Central Analytical Laboratories (CAL) at the Egyptian Petroleum Research Institute (EPRI), during the experimental research studies.

Conflicts of Interest: The authors declare no conflict of interest. The funders had no role in the study’s design, in the collection, analyses, or interpretation of data, in the writing of the manuscript, or in the decision to publish the results.

References

1. Karaman, C.; Karaman, O.; Show, P.L.; Orooji, Y.; Karimi-Maleh, H. Utilization of a double-cross-linked amino-functionalized three-dimensional graphene networks as a monolithic adsorbent for methyl orange removal: Equilibrium, kinetics, thermodynamics and artificial neural network modeling. *Environ. Res.* **2022**, *207*, 112156. [[CrossRef](#)] [[PubMed](#)]
2. Patni, H.; Ragunathan, B. Recycling and Re-Usage of Oilfield Produced Water—A Review. *Mater. Today Proc.* **2023**, *77*, 307–313. [[CrossRef](#)]
3. Younis, S.A.; Maitlo, H.A.; Lee, J.; Kim, K.H. Nanotechnology-Based Sorption and Membrane Technologies for the Treatment of Petroleum-Based Pollutants in Natural Ecosystems and Wastewater Streams. *Adv. Colloid Interface Sci.* **2020**, *275*, 102071. [[CrossRef](#)] [[PubMed](#)]
4. Ghobashy, M.M.; Younis, S.A.; Elhady, M.A.; Serp, P. Radiation Induced In-Situ Cationic Polymerization of Polystyrene Organogel for Selective Absorption of Cholorophenols from Petrochemical Wastewater. *J. Environ. Manag.* **2018**, *210*, 307–315. [[CrossRef](#)]
5. Zhao, C.; Zhou, J.; Yan, Y.; Yang, L.; Xing, G.; Li, H.; Wu, P.; Wang, M.; Zheng, H. Application of Coagulation/Flocculation in Oily Wastewater Treatment: A Review. *Sci. Total Environ.* **2021**, *765*, 142795. [[CrossRef](#)]
6. Moremada, P.; Kalpage, S. Advances in Coagulation Technique for COD Removal of Petroleum Wastewater—A Review. In *International Conference on Sustainable Built Environment*; Springer: Berlin/Heidelberg, Germany, 2023; pp. 733–747.
7. Malik, M.; Ibrahim, S.M.; Nazir, M.A.; Tahir, A.A.; Tufail, M.K.; Shah, S.S.A.; Anum, A.; Wattoo, M.A.; Rehman, A.U. Engineering of a Hybrid g-C₃N₄/ZnO-W/Co_x Heterojunction Photocatalyst for the Removal of Methylene Blue Dye. *Catalysts* **2023**, *13*, 813. [[CrossRef](#)]
8. Jiang, J.-Q. The Role of Coagulation in Water Treatment. *Curr. Opin. Chem. Eng.* **2015**, *8*, 36–44. [[CrossRef](#)]
9. Wei, H.; Gao, B.; Ren, J.; Li, A.; Yang, H. Coagulation/Flocculation in Dewatering of Sludge: A Review. *Water Res.* **2018**, *143*, 608–631. [[CrossRef](#)]
10. Jasmine, J.; Mukherji, S. Characterization of Oily Sludge from a Refinery and Biodegradability Assessment Using Various Hydrocarbon Degrading Strains and Reconstituted Consortia. *J. Environ. Manag.* **2015**, *149*, 118–125. [[CrossRef](#)]
11. Aljuboury, D.; Palaniandy, P.; Abdul Aziz, H.B.; Feroz, S. Treatment of Petroleum Wastewater by Conventional and New Technologies—A Review. *Glob. Nest J.* **2017**, *19*, 439–452.
12. Lapointe, M.; Barbeau, B. Understanding the Roles and Characterizing the Intrinsic Properties of Synthetic vs. Natural Polymers to Improve Clarification through Interparticle Bridging: A Review. *Sep. Purif. Technol.* **2020**, *231*, 115893. [[CrossRef](#)]

13. Lapointe, M.; Papineau, I.; Peldszus, S.; Peleato, N.; Barbeau, B. Identifying the Best Coagulant for Simultaneous Water Treatment Objectives: Interactions of Mononuclear and Polynuclear Aluminum Species with Different Natural Organic Matter Fractions. *J. Water Process Eng.* **2021**, *40*, 101829. [[CrossRef](#)]
14. Wei, N.; Zhang, Z.; Liu, D.; Wu, Y.; Wang, J.; Wang, Q. Coagulation Behavior of Polyaluminum Chloride: Effects of PH and Coagulant Dosage. *Chin. J. Chem. Eng.* **2015**, *23*, 1041–1046. [[CrossRef](#)]
15. Sudoh, R.; Islam, M.S.; Sazawa, K.; Okazaki, T.; Hata, N.; Taguchi, S.; Kuramitz, H. Removal of Dissolved Humic Acid from Water by Coagulation Method Using Polyaluminum Chloride (PAC) with Calcium Carbonate as Neutralizer and Coagulant Aid. *J. Environ. Chem. Eng.* **2015**, *3*, 770–774. [[CrossRef](#)]
16. Zhang, Z.; Jing, R.; He, S.; Qian, J.; Zhang, K.; Ma, G.; Chang, X.; Zhang, M.; Li, Y. Coagulation of Low Temperature and Low Turbidity Water: Adjusting Basicity of Polyaluminum Chloride (PAC) and Using Chitosan as Coagulant Aid. *Sep. Purif. Technol.* **2018**, *206*, 131–139. [[CrossRef](#)]
17. Chen, Y.; Matsui, Y.; Sato, T.; Shirasaki, N.; Matsushita, T. Overlooked Effect of Ordinary Inorganic Ions on Polyaluminum-Chloride Coagulation Treatment. *Water Res.* **2023**, *235*, 119909. [[CrossRef](#)]
18. Satish Reddy, M.; Neeraja, D. Aluminum Residue Waste for Possible Utilisation as a Material: A Review. *Sādhanā* **2018**, *43*, 124. [[CrossRef](#)]
19. Ghulam, N.A.; Abbas, M.N.; Sachit, D.E. Preparation of Synthetic Alumina from Aluminium Foil Waste and Investigation of Its Performance in the Removal of RG-19 Dye from Its Aqueous Solution. *Indian Chem. Eng.* **2020**, *62*, 301–313. [[CrossRef](#)]
20. Gautam, M.; Pandey, B.; Agrawal, M. Carbon footprint of aluminum production: Emissions and mitigation. In *Environmental Carbon Footprints*; Butterworth-Heinemann: Oxford, UK, 2018; pp. 197–228. [[CrossRef](#)]
21. Deena, H.; Khadeejah, P.; Leena, P.K.F.; Lekshmi, J.S.; Sreekumar, N. Production of Industrial Coagulant (Poly Aluminium Chloride) from Used Beverage Cans. *J. Sci. Ind. Res.* **2019**, *78*, 448–453.
22. Srivastava, V.C.; Mall, I.D.; Mishra, I.M. Treatment of Pulp and Paper Mill Wastewaters with Poly Aluminium Chloride and Bagasse Fly Ash. *Colloids Surf. A Physicochem. Eng. Asp.* **2005**, *260*, 17–28. [[CrossRef](#)]
23. Kong, Y.; Ma, Y.; Ding, L.; Ma, J.; Zhang, H.; Chen, Z.; Shen, J. Coagulation Behaviors of Aluminum Salts towards Humic Acid: Detailed Analysis of Aluminum Speciation and Transformation. *Sep. Purif. Technol.* **2021**, *259*, 118137. [[CrossRef](#)]
24. Chen, W.; Li, B.; Li, Q.; Tian, J. Effect of Polyaluminum Chloride on the Properties and Hydration of Slag-Cement Paste. *Constr. Build. Mater.* **2016**, *124*, 1019–1027. [[CrossRef](#)]
25. Zhuang, J.; Qi, Y.; Yang, H.; Li, H.; Shi, T. Preparation of Polyaluminum Zirconium Silicate Coagulant and Its Performance in Water Treatment. *J. Water Process Eng.* **2021**, *41*, 102023. [[CrossRef](#)]
26. Zhou, F.S.; Hu, B.; Cui, B.L.; Liu, F.B.; Liu, F.; Wang, W.H.; Liu, Y.; Lu, R.R.; Hu, Y.M.; Zhang, Y.H.; et al. Preparation and Characteristics of Polyaluminium Chloride by Utilizing Fluorine-Containing Waste Acidic Mother Liquid from Clay-Brine Synthetic Cryolite Process. *J. Chem.* **2014**, *2014*, 274126. [[CrossRef](#)]
27. Kloprogge, J.T.; Ruan, H.; Frost, R.L. Near-Infrared Spectroscopic Study of Basic Aluminum Sulfate and Nitrate. *J. Mater. Sci.* **2001**, *36*, 603–607. [[CrossRef](#)]
28. Lal, K.; Garg, A. Physico-Chemical Treatment of Pulping Effluent: Characterization of Flocs and Sludge Generated after Treatment. *Sep. Sci. Technol.* **2017**, *52*, 1583–1593. [[CrossRef](#)]
29. Tzoupanos, N.D.; Zouboulis, A.I.; Tsoleridis, C.A. A Systematic Study for the Characterization of a Novel Coagulant (Polyaluminium Silicate Chloride). *Colloids Surf. A Physicochem. Eng. Asp.* **2009**, *342*, 30–39. [[CrossRef](#)]
30. Shoaib, A.G.M.; El-sikaily, A.; Nemr, A.E. *Testing the Carbonization Condition for High Surface Area Preparation of Activated Carbon Following Type IV Green Alga Ulva Lactuca*; Springer: Berlin/Heidelberg, Germany, 2022; pp. 3303–3318.
31. Yurdakal, S.; Garlisi, C.; Özcan, L.; Bellardita, M.; Palmisano, G. (*Photo*)Catalyst Characterization Techniques: Adsorption Isotherms and BET, SEM, FTIR, UV-Vis, Photoluminescence, and Electrochemical Characterizations in Heterogeneous Photocatalysis; Elsevier: Amsterdam, The Netherlands, 2019; pp. 87–152. [[CrossRef](#)]
32. Zhao, A.C.; Zhang, T.A.; Lv, G.Z. Thermodynamic Analysis of Nucleation during Pyrolysis Process of Aluminum Chloride Solution. *MRS Commun.* **2021**, *11*, 679–684. [[CrossRef](#)]
33. Shi, B.; Wei, Q.; Wang, D.; Zhu, Z.; Tang, H. Coagulation of Humic Acid: The Performance of Preformed and Non-Preformed Al Species. *Colloids Surf. A Physicochem. Eng. Asp.* **2007**, *296*, 141–148. [[CrossRef](#)]
34. Klimiuk, E.; Filipkowska, U.; Korzeniowska, A. Effects of PH and Coagulant Dosage on Effectiveness of Coagulation of Reactive Dyes from Model Wastewater by Polyaluminium Chloride (PAC). *Pol. J. Environ. Stud.* **1999**, *8*, 73–79.
35. Liang, L.; Tan, J.; Peng, Y.; Xia, W.; Xie, G. The Role of Polyaluminum Chloride in Kaolinite Aggregation in the Sequent Coagulation and Flocculation Process. *J. Colloid Interface Sci.* **2016**, *468*, 57–61. [[CrossRef](#)] [[PubMed](#)]
36. Wu, Z.; Zhang, X.; Pang, J.; Li, J.; Li, J.; Zhang, P. High-Poly-Aluminum Chloride Sulfate Coagulants and Their Coagulation Performances for Removal of Humic Acid. *RSC Adv.* **2020**, *10*, 7155–7162. [[CrossRef](#)] [[PubMed](#)]
37. Wang, Z.; Peng, S.; Nan, J.; He, C.; Qi, F.; Ji, X.; Li, W.; Sun, D. Effect of Al Species of Polyaluminum Chlorides on Floc Breakage and Re-Growth Process: Dynamic Evolution of Floc Properties, Dissolved Organic Matter and Dissolved Al. *Chemosphere* **2020**, *249*, 126449. [[CrossRef](#)]
38. Zand, A.D.; Hoveidi, H. Comparing Aluminium Sulfate and Poly-Aluminium Chloride (PAC) Performance in Turbidity Removal from Synthetic Water. *J. Appl. Biotechnol. Rep.* **2015**, *2*, 287–292.

39. Pernitsky, D.J.; Edzwald, J.K. Selection of alum and polyaluminum coagulants: Principles and applications. *J. Water Supply: Res. Technol.-AQUA* **2006**, *55*, 121–141. [[CrossRef](#)]
40. Zhan, X.; Gao, B.; Yue, Q.; Wang, Y.; Wang, Q. Coagulation Efficiency of Polyaluminum Chloride for Natural Organic Matter Removal from Low Specific UV Absorbance Surface Water and the Subsequent Effects on Chlorine Decay. *Chem. Eng. J.* **2010**, *161*, 60–67. [[CrossRef](#)]
41. Abuazar, M.S.S.; Karaağaç, S.U.; Abu Amr, S.S.; Alazaiza, M.Y.D.; Bashir, M.J. Recent Advancement in the Application of Hybrid Coagulants in Coagulation-Flocculation of Wastewater: A Review. *J. Clean. Prod.* **2022**, *345*, 131133. [[CrossRef](#)]
42. Deng, S.; Zhou, Q.; Yu, G.; Huang, J.; Fan, Q. Removal of Perfluorooctanoate from Surface Water by Polyaluminium Chloride Coagulation. *Water Res.* **2011**, *45*, 1774–1780. [[CrossRef](#)]
43. Djeffal, K.; Bouranene, S.; Fievet, P.; Déon, S.; Gheid, A. Treatment of Controlled Discharge Leachate by Coagulation-Flocculation: Influence of Operational Conditions. *Sep. Sci. Technol.* **2021**, *56*, 168–183. [[CrossRef](#)]
44. Wu, C.-D.; Xu, X.-J.; Liang, J.-L.; Wang, Q.; Dong, Q.; Liang, W.-L. Enhanced Coagulation for Treating Slightly Polluted Algae-Containing Surface Water Combining Polyaluminum Chloride (PAC) with Diatomite. *Desalination* **2011**, *279*, 140–145. [[CrossRef](#)]
45. Mohammed, T.J.; Shakir, E. Effect of Settling Time, Velocity Gradient, and Camp Number on Turbidity Removal for Oilfield Produced Water. *Egypt. J. Pet.* **2018**, *27*, 31–36. [[CrossRef](#)]
46. You, Z.; Xu, H.; Sun, Y.; Zhang, S.; Zhang, L. Effective Treatment of Emulsified Oil Wastewater by the Coagulation–Flotation Process. *RSC Adv.* **2018**, *8*, 40639–40646. [[CrossRef](#)]
47. Nan, J.; Wang, Z.; Yao, M.; Yang, Y.; Zhang, X. Characterization of Re-Grown Floc Size and Structure: Effect of Mixing Conditions during Floc Growth, Breakage and Re-Growth Process. *Environ. Sci. Pollut. Res.* **2016**, *23*, 23750–23757. [[CrossRef](#)] [[PubMed](#)]
48. Wang, Z.; Nan, J.; Yao, M.; Yang, Y. Effect of Additional Polyaluminum Chloride and Polyacrylamide on the Evolution of Floc Characteristics during Floc Breakage and Re-Growth Process. *Sep. Purif. Technol.* **2017**, *173*, 144–150. [[CrossRef](#)]

Disclaimer/Publisher's Note: The statements, opinions and data contained in all publications are solely those of the individual author(s) and contributor(s) and not of MDPI and/or the editor(s). MDPI and/or the editor(s) disclaim responsibility for any injury to people or property resulting from any ideas, methods, instructions or products referred to in the content.